AN *IN VITRO* COMPARATIVE STUDY OF [^{14}C]-EUGENOL AND [^{14}C]-METHYLEUGENOL ACTIVATION AND DETOXIFICATION KINETICS IN HUMAN, MOUSE, AND RAT LIVER FRACTIONS

Emmanuel MINET[1], Gentile Daniela[2], Clive Meredith[1], Eian D. Massey[1]
[1]British American Tobacco, Group R&D, Southampton, UK,
[2]Charles River Laboratories, Edinburgh, UK

Introduction - Eugenol is a natural alkenylbenzene compound used in a variety of consumer products including Kretek cigarettes. There is limited evidence for the carcinogenicity of eugenol to experimental animals. However, *in vitro* tests for the genotoxic potential of eugenol have on occasion reported a positive result. In contrast, the structurally related alkenylbenzene methyleugenol is consistently reported as genotoxic and carcinogenic *in vitro* and *in vivo*. The absence of unequivocal translation of toxicity data obtained from animal models to human is a limiting factor for eugenol toxicity assessment.

Metabolism of Alkenylbenzenes (Figure 1) - Bioactive alkenylbenzene metabolites are the products of a genotoxic and a cytotoxic pathway:
The genotoxic pathway involves two steps with first, a limiting 1'-hydroxylation step (proximate carcinogen), followed by sulfation of the 1'-hydroxyl and formation of a genotoxic carbocation (ultimate carcinogen) (**Figure 1**) (Boberg *et al.* 1983; Burkey *et al.* 2000).
The cytotoxic pathway consists of a deprotonation yielding a cytotoxic quinone methide (**Figure 1**) (Thompson *et al.* 1990).
The proposed protective mechanism for detoxification of alkenylbenzenes involves phenolic glucuronidation (**Figure 1**).

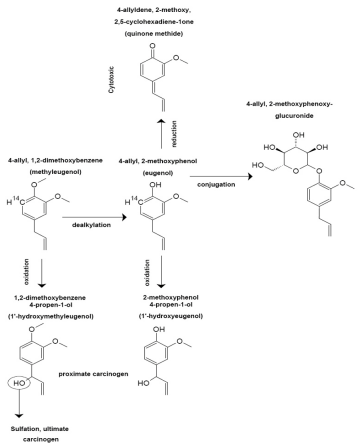

Figure 1: proposed metabolic pathways for eugenol and methyleugenol

Objective -The objective of this study was to compare the kinetics of phase I and phase II metabolism in the bioactivation and detoxification of eugenol and methyleugenol in different species. The metabolic routes of [^{14}C]-eugenol and [^{14}C]-methyleugenol were investigated in human, rat, and mouse, using *in vitro* hepatic subcellular fractions. The formation of the 1'-hydroxy proximate carcinogen and the cytotoxic quinone methide were quantified and kinetic parameters ($_{app}$Km and $_{app}$Vmax) were calculated. In this report we describe how oxidative and conjugative pathways contribute to the distinct metabolic fate of eugenol and methyleugenol in humans and how this compares to rodents.

Oxidative metabolism in hepatic microsomes – kinetic experiments for [^{14}C]-eugenol and [^{14}C]-methyleugenol activation were performed to establish the corresponding $_{app}$Km and $_{app}$Vmax values for 1'-oxidation (**Figure 2**) and covalent binding (**Figure 3**) in rodent and human liver microsomes.

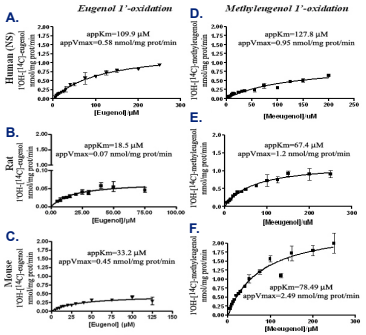

Figure 2: Formation rate of 1'-hydroxy-[^{14}C]-eugenol in human (**A**), rat (**B**) and mouse (**C**) hepatic microsomes at increasing concentrations of [^{14}C]-eugenol [Eugenol] (5-250 µM). Formation rate of 1'-hydroxy-[^{14}C]-methyleugenol in human (**D**), rat (**E**), and mouse (**F**) hepatic microsomes at increasing concentrations of [^{14}C]-methyleugenol [Meeugenol] (5-250 µM). Results are presented as mean ± SD for independent triplicates.

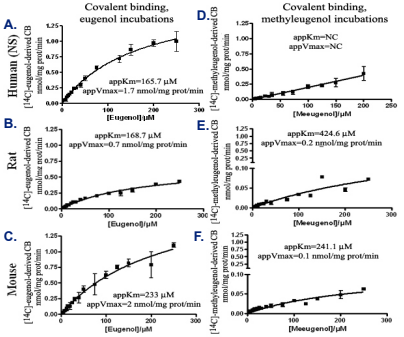

Figure 3: Formation rate of covalent binding metabolite(s) of [^{14}C]-eugenol in human (**A**), rat (**B**) and mouse (**C**) hepatic microsomes at increasing concentrations of [^{14}C]-eugenol [Eugenol] (5-250 µM). Formation rate of covalent binding metabolite(s) of [^{14}C]-methyleugenol in human (**D**), rat (**E**), and mouse (**F**) hepatic microsomes at increasing concentrations of [^{14}C]-methyleugenol [Meeugenol] (5-250 µM). Results are presented as mean ± SD for independent triplicates.

Kinetic comparison of phase II conjugation in hepatic S9 – In a second set of experiments the formation of the phenoxy-glucuronide (**Figure 4, 5**) and dealkylation (**Figure 5**) were quantified following incubation of [^{14}C]-eugenol and [^{14}C]-methyleugenol with hepatic S9 fractions and cofactors.

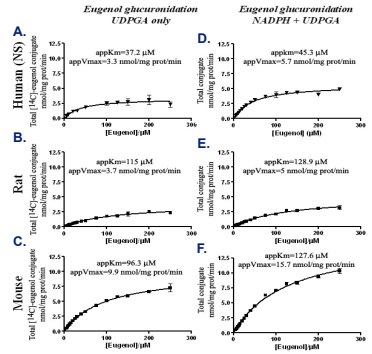

Figure 4: Formation rate of [^{14}C]-eugenol glucuronide conjugate. Increasing concentrations (5-250 µM) of [^{14}C]-eugenol [Eugenol] were incubated with UDPGA in human (**A**), rat (**B**), and mouse (**C**) S9 fractions and formation of 4-allyl, 2-[^{14}C]-methoxyphenoxy glucuronide was quantified. An other incubation was conducted with NADPH +UDPGA in human (**D**), rat (**E**), and mouse (**F**) hepatic S9 and formation of total conjugate was recorded. Results are presented as mean ± SD for independent triplicates.

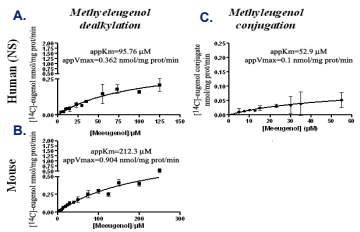

Figure 5: Formation rate of [^{14}C]-eugenol at increasing concentrations (5-250 µM) of [^{14}C]-methyleugenol [Meeugenol] in human (**A**), and rat (**B**) hepatic microsomes incubated with NADPH. (**C**) Formation rate of [^{14}C]-eugenol glucuronide conjugate following incubation of [^{14}C]-methyleugenol [Meeugenol] (5-250 µM) with NADPH+UDPGA in human hepatic microsomes. Results are presented as mean ± SD for independent triplicates.

Competition between oxidation and conjugation – [^{14}C]-eugenol and [^{14}C]-methyleugenol were co-incubated with NADPH and UDPGA to assess the dynamic of oxidation *vs* conjugation. [^{14}C]-eugenol conjugation is the favored pathway while 1'-hydroxylation is the main reaction for methyleugenol.

species	cofactors	1'-OHeugenol	eugenol CB	1'-OHmethyleugenol	methyleugenol CB
Human	NADPH	3.7% ± 0.2	7.2% ± 0.3	34.7% ± 0.6	2.0% ± 0.2
	NADPH+UDPGA	**no peak**	**0.9% ± 0.01**	34.3% ± 0.9	1.2% ± 0.2
Mouse	NADPH	15.4% ± 0.7	1.2% ± 0.3	54.7% ± 3.2	1.06% ± 0.1
	NADPH+UDPGA	**no peak**	**0.3% ± 0.04**	64.1% ± 1.7	0.3% ± 0.06
Rat	NADPH	9.8% ± 0.7	3.1% ± 0.05	39.0% ± 2.0	0.5% ± 0.1
	NADPH+UDPGA	6.1% ± 0.4	1.9% ± 0.03	40.3% ± 0.1	0.5% ± 0.2

Table 1: Relative percentage of 1'-hydroxy (1'-OH) and covalently bound (CB) [^{14}C]-eugenol and [^{14}C]-methyleugenol metabolites following incubation with human, mouse, and rat hepatic S9 fractions with NADPH ± UDPGA. Results for each metabolite are expressed as relative percentage (%) of starting substrate dose ± SD for independent triplicates. Key changes following addition of UDPGA are highlighted in grey.

Conclusion - Overall, we have compared the *in vitro* metabolism of [^{14}C]-eugenol and [^{14}C]-methyleugenol in hepatic fractions in three species. Based on co-chromatography there did not appear to be any species specific metabolites formed although the relative rates of formation differed quite significantly.

Our results show that methyleugenol generates a significant amount of the 1'-hydroxy proximate carcinogen while eugenol glucuronidation prevents the formation of both 1'-hydroxyeugenol and the quinone methide. Comparative kinetics confirm the relative formation rate for each metabolite and the contribution of each metabolic pathways has been summarized in **Figure 6** according to the catalytic efficiencies.

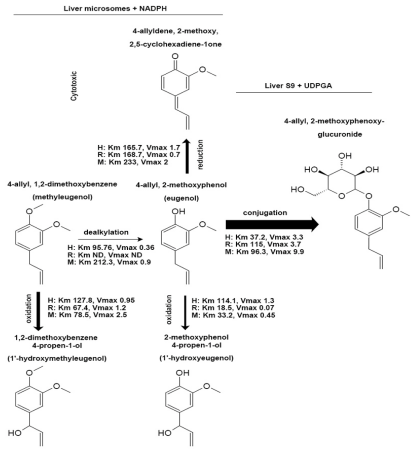

Figure 6: Proposed metabolic pathways of eugenol and methyleugenol activation and conjugation showing the relative weight of each reaction in liver according to the determined kinetics parameters.

References
Boberg,E.W., Miller,E.C., Miller,J.A., Poland,A., and Liem,A. (1983). Strong evidence from studies with brachymorphic mice and pentachlorophenol that 1'-sulfooxysafrole is the major ultimate electrophilic and carcinogenic metabolite of 1'-hydroxysafrole in mouse liver. *Cancer Res.* 43, 5163-5173.
Burkey,J.L., Sauer,J.M., McQueen,C.A., and Sipes,I.G. (2000). Cytotoxicity and genotoxicity of methyleugenol and related congeners-- a mechanism of activation for methyleugenol. *Mutat. Res.* 453, 25-33.
Thompson,D., Constantin-Teodosiu,D., Egestad,B., Mickos,H., and Moldeus,P. (1990). Formation of glutathione conjugates during oxidation of eugenol by microsomal fractions of rat liver and lung. *Biochem. Pharmacol.* 39, 1587-1595.